

Cold inelastic collisions between lithium and cesium in a two-species magneto-optical trap

U. Schlöder^a, H. Engler, U. Schünemann^b, R. Grimm, and M. Weidemüller^c

Max-Planck-Institut für Kernphysik, 69029 Heidelberg, Germany

submitted to Euro. Phys. J. D, special issue on “Laser Cooling and Trapping”, December 1998

Abstract. We investigate collisional properties of lithium and cesium which are simultaneously confined in a combined magneto-optical trap. Trap-loss collisions between the two species are comprehensively studied. Different inelastic collision channels are identified, and inter-species rate coefficients as well as cross sections are determined. It is found that loss rates are independent of the optical excitation of Li, as a consequence of the repulsive Li*-Cs interaction. Li and Cs loss by inelastic inter-species collisions can completely be attributed to processes involving optically excited cesium (fine-structure changing collisions and radiative escape). By lowering the trap depth for Li, an additional loss channel of Li is observed which results from ground-state Li-Cs collisions changing the hyperfine state of cesium.

PACS. 34.50.Rk Laser-modified scattering and reactions – 32.80.Pj Optical cooling; trapping

1 Introduction

Cold collisions between trapped, laser-cooled atoms have been the subject of extensive research in the past years [1]. In contrast to collisions of thermal atoms, the collision process between cold atoms is extremely sensitive to the long-range part of the inter-atomic interaction allowing precise determination of molecular potentials [2] and atomic lifetimes [3]. In the presence of light fields, molecular excitation during the collisional process is non-negligible, leading to phenomena such as light-induced collisions [4,5], photoassociation [2], optical shielding of inelastic processes [6] and formation of cold ground-state molecules [7].

Investigations have almost exclusively concentrated on binary collisions between atoms of the same species [1,8]. Light-induced cold collisions between two different species (*heteronuclear* collisions) strongly differ from single-species collisions (*homonuclear* collisions). The excited-state interaction potential for two different species is of much shorter range (van-der-Waals potential $\propto 1/R^6$ at large interatomic separations R) than the excited state potential for two atoms of the same species (resonant-dipole potential $\propto 1/R^3$). In the homonuclear case, the duration of the cold collision is much longer than the excited-state lifetimes [9] so that the dynamics of the collisional process greatly depends on the atom-light interaction during the

collision process. For the heteronuclear case, even a cold collision takes less time than the lifetimes of the excited atomic states. The collision process is therefore essentially determined by the asymptotic states which are initially prepared, much like classical “hot” collisions.

However, the low temperatures of laser-cooled atoms lead to a large extension of the molecular wavepacket formed during the cold collision. The wavepacket spreads over typically some fraction of an optical wavelength which is of the same order of magnitude as the range of the interaction potentials. A light-induced cold collision between two different species is therefore highly quantum-mechanical with mainly the s-wave scattering distribution determining the cross-section, in contrast to homonuclear collisions involving excited atoms [10].

Only recently, simultaneous trapping of two different atomic species has been reported [11,12,13]. In this article, we present the first investigation on inelastic cold collisions between lithium and cesium, i.e. the lightest and the heaviest stable alkali. This extreme combination opens intriguing perspectives for future experiments related to the large difference in mass and electron affinity of the two atomic species, e.g., sympathetic cooling of lithium by optically cooled cesium [14] and the formation of cold polar molecules with large electric dipole moment which could be trapped electrostatically [15]. In our experiments, both species are simultaneously confined in a combined magneto-optical trap. Trap loss is studied by analyzing the decay of the trapped particle number after interruption of the loading flux, both in presence and in absence of the other species. By choosing appropriate trap parameters, different trap loss processes based on inelastic colli-

^a Present address: Physikalisches Institut, Eberhard-Karls-Universität, 72076 Tübingen, Germany

^b Present address: BASF AG, DWL/LP - L426, 67056 Ludwigshafen, Germany

^c e-mail: m.weidemueeller@mpi-hd.mpg.de

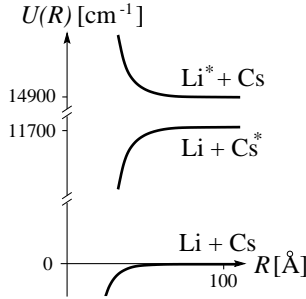


Fig. 1. Long-range interaction energies plotted schematically as a function of internuclear distance for the ground and first excited states of lithium and cesium.

sions between lithium and cesium are identified, and the corresponding cross sections and rate coefficients are determined.

The specific features of inelastic cold collisions between two different species are introduced in Sec. 2 with emphasis on the peculiarities of the Li-Cs system. The combined magneto-optical trap for simultaneous confinement of lithium and cesium is described in Sec. 3. In Sec. 4 detailed quantitative studies of trap loss through inelastic Li-Cs collisions are presented. Sec. 5 summarizes the main results.

2 Two-species cold collisions

2.1 Quasi-molecular potentials

When two cold atoms approach each other, the interaction between the atoms leads to the formation of quasi-molecular states. The leading term in the long-range part of the interaction arises from the dipole-dipole interaction. If both atoms are in their ground state, the potential energy is given by the well-known van-der-Waals expression $W_{gg} = C_6/R^6$. The coefficient C_6 can be estimated by treating the two atoms A and B as simple two-level systems with transition frequencies $\omega_i = 2\pi c/\lambda_i$ and electric dipole moments d_i ($i = A$ or B). Second-order perturbation theory yields

$$C_6 \simeq -\frac{4d_A^2 d_B^2}{\hbar(\omega_A + \omega_B)}. \quad (1)$$

The van-der-Waals interaction between two ground state atoms is thus always attractive as shown in Fig. 1.

If one collision partner arrives in an excited state, the nature of the interaction depends on whether both atoms belong to the same species, or whether two different species collide. For the homonuclear quasi-molecule, the interaction potential is given by the resonant-dipole interaction $W_{ge} = C_3^*/R^3$ with the perturbative two-level result $C_3^* \simeq \pm 2d^2$. In the heteronuclear case with atom A in the excited state and atom B in the ground state, one obtains a van-der-Waals potential $W_{ge} = C_6^*/R^6$ with

$$C_6^* \simeq \frac{4d_A^2 d_B^2}{\hbar(\omega_A - \omega_B)}. \quad (2)$$

The relative value of the transition energies determines the character of the interaction. If the collision partner with the larger (smaller) resonance frequency is excited, the interaction is generally repulsive (attractive) as indicated in Fig. 1 for the case of lithium and cesium. As we will see, this general feature of the excited state van-der-Waals interaction has important implications on the collisional properties of two different species.

The van-der-Waals coefficients C_6 and C_6^* differ by the factor $(\omega_A - \omega_B)/(\omega_A + \omega_B) \ll 1$ resulting in a much steeper potential for the excited state than for the ground state (see Fig. 1). Although the two-level approximation is an oversimplified model for the complex level schemes of real atoms, the numerical values for the coefficients C_6 , C_3^* and C_6^* derived from the two-level approach reproduce the right orders of magnitude for alkali dimers. For more accurate determination of the long-range molecular potentials, elaborate models including spin-orbit effects and interacting molecular states have been developed [16].

2.2 Inelastic processes

Inelastic collisions in a trap lead to loss of atoms when the kinetic energy gain of the colliding atom is larger than the trap depth. If the energy gain is smaller than the trap depth, the atom is retained in the trap, but the inelastic collision represents a significant heating mechanism. Due to the low temperatures achieved in a magneto-optical trap (MOT), the initial kinetic energy of the collision partners can be neglected with respect to the interaction energy. In the presence of light fields, two basic processes were identified for cold inelastic collisions involving optical excitation of the colliding pair [10,17]: fine-structure changing collisions (FC) and radiative escape (RE). For two different species, an exoergic energy-exchange reaction $A^* + B \rightarrow A + B^* + \hbar(\omega_A - \omega_B)$ may also take place. Due to the repulsive A^*-B potential and the large energy defect associated with this reaction as compared to other inelastic processes, we conjecture that this process has negligible influence.

When a photon from the light field is absorbed during the collision, the colliding partners are accelerated towards each other on the strongly attractive potential of the excited state. The FC mechanism is based on coupling of the excited molecular state to another fine-structure or hyperfine-structure state with lower asymptotic energy, which occurs at typical distances smaller 10 \AA . The kinetic energy gain of the atom pair is the difference between the absorbed photon energy and the energy of the lower excited fine-structure state. The RE mechanism relies on the spontaneous emission of a photon during acceleration on the excited molecular potential. The gain of kinetic energy is then given by the difference in energy between the absorbed and the emitted photon.

Both mechanisms involve one collision partner in the excited state. The excitation probability of the collisional quasi-molecule is largest when the detuning δ of the light field from the atomic resonance is compensated by the interaction energy. The corresponding internuclear distance

is called the Condon point R_C defined by the condition $W_{ge}(R_C) - W_{gg}(R_C) = \hbar\delta$. For typical detunings of a MOT ($\delta = -(1-6)\Gamma$, with Γ denoting the inverse lifetime of the excited state), the Condon point has values around $500 - 2000 \text{ \AA}$ for homonuclear collisions with the long-range $1/R^3$ resonant-dipole potential, and much smaller values around $50 - 150 \text{ \AA}$ for heteronuclear collisions with the shorter-range $1/R^6$ excited state van-der-Waals potential. At distances smaller than the Condon point, the colliding atoms quickly decouple from the light field due to the increasing energy shifts induced by the interatomic interaction. Taking typical relative velocities $\bar{v} = 0.1 - 1 \text{ m/s}$ in a MOT and typical radiative lifetimes $\Gamma^{-1} \simeq 30 \text{ ns}$, the semiclassical probability of reaching small internuclear distances on an excited state molecular potential (“survival probability”) is small for homonuclear collisions, but might get close to unity for heteronuclear ones.

In addition to the excited-state inelastic collisions, collisions involving both colliding atoms in the ground state may occur. In particular, hyperfine-changing collisions (HFC) releasing the ground state hyperfine energy, similar to the FC mechanism in the excited state, can play a role for losses in shallow traps.

2.3 Cold lithium-cesium collisions

The special case of a cold Li-Cs collision shows some peculiar features. The lithium and cesium level schemes for the ground and first excited states are shown in Fig. 2. Lifetimes for the Li and Cs excited states are $(\Gamma_{\text{Li}})^{-1} = 27 \text{ ns}$ and $(\Gamma_{\text{Cs}})^{-1} = 30 \text{ ns}$, respectively. The $S_{1/2} - P_{3/2}$ transitions ($D2$ line) at 671 nm for Li and 852 nm for Cs are used for cooling and trapping. Due to the difference in transition energy, the quasi-molecular potential for a Li-Cs collision is repulsive for *all* substates with $\text{Li}^* + \text{Cs}$ asymptotes, and attractive for *all* substates with $\text{Li} + \text{Cs}^*$ asymptotes [16] as indicated in Fig. 1. The repulsive long-range interaction for the $\text{Li}^* - \text{Cs}$ pair has already experimentally been demonstrated by spectroscopic measurements in a hot Li-Cs vapor [18]. Due to the small initial kinetic energy with respect to the interatomic interaction potential, a $\text{Li}^* - \text{Cs}$ pair is prevented from reaching small internuclear separations where inelastic processes can occur.

Possible inelastic channels for Li-Cs collisions are therefore hyperfine-changing collisions for ground state Li and Cs, as well as FC, HFC and RE collisions involving Cs^* . Momentum and energy conservation require that only 5%, i.e. $m_{\text{Li}}/(m_{\text{Li}} + m_{\text{Cs}})$ ($m_i = \text{mass of the atoms}$), of the released energy is transferred to the heavier collision partner Cs. When the two-species MOT is optimized for maximum capture velocity for each species (trap depth $\sim h \times 15 \text{ GHz}$ with $h = \text{Planck's constant}$), Li loss is induced by Cs when the total energy release is larger than $\sim h \times 16 \text{ GHz}$, while the energy release for Li-induced Cs loss has to be larger than $\sim h \times 300 \text{ GHz}$. The hyperfine splittings of Li, Li^* , Cs and Cs^* are therefore too small to induce trap loss. However, for a slightly shallower Li-MOT, the hyperfine energy of the ground-state Cs may just be sufficient to

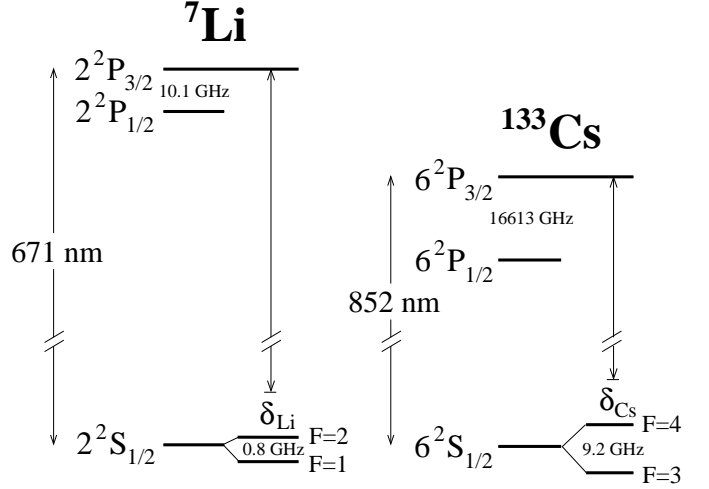


Fig. 2. Level schemes for the ground and first excited states for lithium and cesium.

induce loss of Li, while the Cs collisions partner remains in the MOT.

With laser cooling, much lower temperatures are achieved for Cs ($\sim 50 \mu\text{K}$) than for Li ($\sim 1 \text{ mK}$), mainly because of the great difference in photon recoil energy $\hbar^2 k^2/m$ with m denoting the mass of the atom and $\hbar k$ the momentum of an absorbed photon. The mean speed for Li atoms at $T_{\text{Li}} = 1 \text{ mK}$ is $\bar{v}_{\text{Li}} = 1.7 \text{ m/s}$. This has to be compared to the mean Cs speed $\bar{v}_{\text{Cs}} = 0.1 \text{ m/s}$ for a Cs temperature of $T_{\text{Cs}} = 50 \mu\text{K}$. The Cs atoms can therefore be considered at rest before the collision, and the mean relative velocity \bar{v}_{LiCs} between cold Li and Cs is solely determined by the Li temperature.

3 Combined cesium-lithium trap

A schematic view of the experiment is presented in Fig. 3. The apparatus is an extension of a MOT for Li which is described in detail in Ref. [19]. The combined magneto-optical trap for lithium *and* cesium consists of three mutually orthogonal pairs of counter-propagating laser beams for each species with opposite circular polarization, intersecting at the center of an axially symmetric magnetic quadrupole field. Field gradients are 14 G/cm along the vertical axis, and 7 G/cm in the horizontal directions. The light field of the MOT is formed by retroreflected beams with a $1/e^2$ -diameter of 15 mm . Total laser power is about 15 mW for the Cs-MOT at 852 nm and 27 mW for the Li-MOT at 671 nm . Completely separated optics is used for the two wavelengths. The same windows are used for each trapping laser beam at 852 nm and 671 nm . The light is coupled into the vacuum chamber with a small angle between the 671 nm -beam and the 852 nm -beam.

The laser beams are provided exclusively by diode lasers. For the trapping of cesium, a diode laser is operated close to the $6S_{1/2}(F=4) \rightarrow 6P_{3/2}(F=5)$ cycling transition

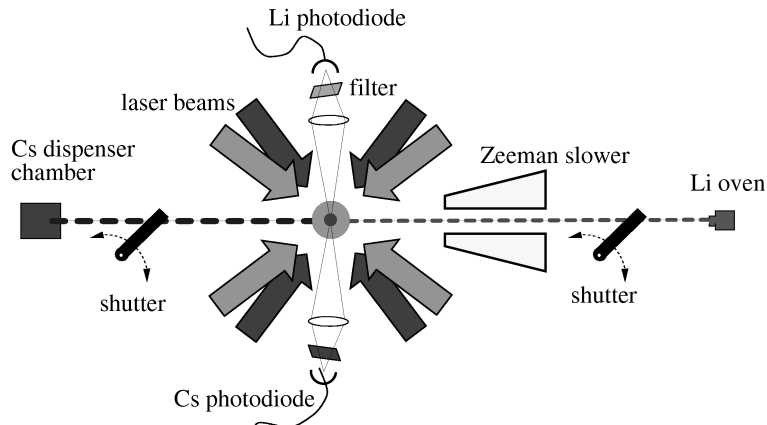


Fig. 3. Experimental setup of the two-species MOT. Not shown are the laser beam for Li deceleration, and the two CCD cameras imaging the trapped atoms from different directions.

of the cesium $D2$ line at 852 nm. To avoid optical pumping into the other hyperfine ground state, a second laser beam from a diode laser resonant with the $6S_{1/2}(F = 3) \rightarrow 6P_{3/2}(F = 4)$ transition is superimposed with the trapping beam. Both lasers are frequency-stabilized relative to absorption lines from Cs vapor cells at room temperature. The error signal of the servo loops is provided by the frequency-dependent circular dichroism of Cs vapor in a glass cell, to which a longitudinal magnetic field of some tens of Gauss is applied. The dichroism is measured as the difference in absorption between the left- and right-circular components of a linearly polarized beam. Trapping of lithium is accomplished with diode lasers in a master-slave injection-locking scheme as described in [19]. The lasers operate close to the $2S_{1/2}(F = 2) \rightarrow 2P_{3/2}$ transition and the $2S_{1/2}(F = 1) \rightarrow 2P_{3/2}$ transition, respectively, of the lithium $D2$ line at 671 nm¹. One of the lasers is locked to Doppler-free absorption lines measured by radio-frequency spectroscopy [21]. The second laser is stabilized with respect to the first by a tunable offset-frequency lock [22].

Both MOTs are loaded from effusive atomic beams which can be interrupted by mechanical shutters (see Fig. 3). The Cs oven at a temperature of typically 85 °C is continuously filled during operation by running a current of ~ 2 A through a set of nine Cs dispensers. The Cs MOT accumulates atoms from the slow velocity tail ($v \leq 10$ m/s) of the Maxwell distribution. Typically, close to 10^6 atoms (at a detuning $\delta_{Cs} = -1.5 \Gamma_{Cs}$) are trapped with a loading time constant of several seconds. Lithium has to be evaporated at much higher temperatures. The small mass of Li results in much higher atom velocities. Atoms with velocity $v \leq 600$ m/s are decelerated in a compact Zeeman slower by an additional laser beam at 671 nm [19]. The trapped atoms are shielded from the Li atomic beam by a small beam block [19]. At a Li oven temperature of 450 °C, the loading rate is around 10^8 atoms/s, yielding up to 10^9

trapped Li atoms. The steady-state number of trapped Li atoms can be adjusted over a wide range by decreasing the loading flux through attenuation of the Zeeman-slowing laser beam. Densities for the Cs and the Li MOT range between 10^9 and 10^{10} atoms/cm³.

The fluorescence of the trapped atoms is monitored by two calibrated photodiodes with narrow-band interference filters at 852 nm and 671 nm, respectively. Shape and position of the two atomic clouds are measured with two CCD cameras. From these measurements, the number of trapped atoms and the density are determined. The cameras are looking from different directions yielding 3D information on the position of the Li and Cs cloud.

The clouds are not necessarily overlapping. To superimpose both clouds, we found it most simple and reproducible to shift the Li onto the Cs cloud by slightly focusing the retroreflected beams at 671 nm and thus introducing a controlled radiation-pressure imbalance. The Li cloud turned out to be more sensitive to a radiation-pressure imbalance than the Cs cloud.

Cooling in the Li-MOT is based on Doppler forces [19], while polarization-gradient forces are acting on the trapped Cs [20]. As a consequence of the different mechanisms, temperatures of the Li cloud in the MOT are above the Doppler temperature ($T_{Li} \approx 1$ mK), while the Cs cloud is cooled to sub-Doppler temperatures ($T_{Cs} \approx 50$ μ K). Fig. 4 shows a fluorescence picture of simultaneously trapped Li and Cs atoms. Due to its much lower temperature the Cs cloud occupies a much smaller volume than the Li cloud, as indicated by the density profiles in Fig. 4. This particular property of the Li/Cs system greatly simplifies quantitative collisional studies.

Binary inelastic collisions between lithium and cesium lead to loss from the two-species MOT. One indication of this loss is a decrease of the steady-state particle number of one species when the other species is also loaded into the combined MOT. In Fig. 5, the temporal evolution of the trapped particle number during loading is shown to illustrate the influence of inter-species collisions. First, only Cs is loaded into the MOT until the steady-state number

¹ The excited-state hyperfine splitting of Li is of the same order as the natural linewidth and can thus not be resolved.

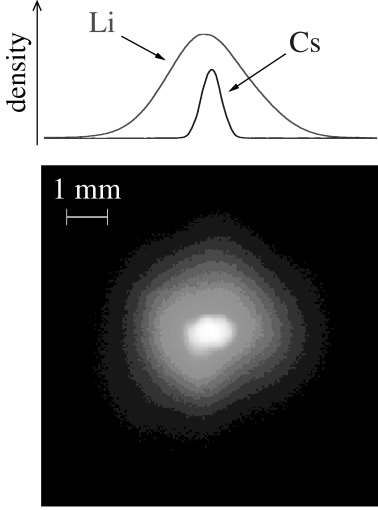


Fig. 4. Camera picture of simultaneously trapped lithium and cesium atoms. The density distributions shown above are measured separately for lithium and cesium using narrow-band filters in front of the CCD camera.

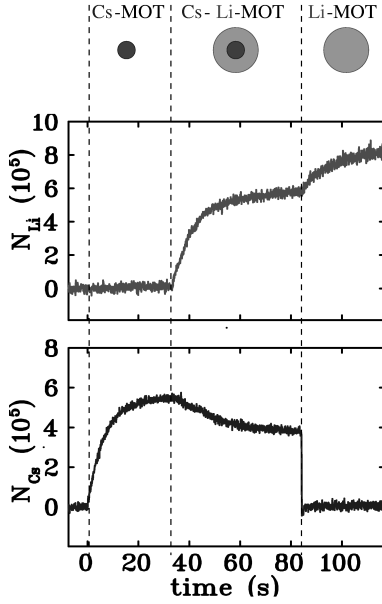


Fig. 5. Temporal evolution of the number of trapped lithium and cesium atoms during loading of the two-species MOT with and without the other species present.

is reached. Then, as Li is also filled into the trap by opening the atomic beam shutter, the number of trapped Cs decreases which indicates inelastic Li-Cs collisions resulting in a trap loss of Cs. After a new steady state has established, loading of Cs is stopped by shuttering the Cs beam, and the light field at 852 nm is interrupted for a short moment, resulting in quick escape of all Cs atoms. Without Cs, the number of trapped Li further increases which shows that inter-species collisions also induce Li loss.

4 Quantitative studies

4.1 Measurement procedures

Inelastic collisions can be studied quantitatively by measuring rate coefficients for the loss of particles from the trap. The temporal evolution of the trapped particle number N_A for the species A under the presence of species B is described by the rate equation

$$\frac{dN_A}{dt} = L_A - \alpha_A N_A - \beta_A \int n_A^2 d^3r - \gamma_{AB} \int n_A n_B d^3r \quad (3)$$

where $n_{A,B}$ denote the local densities and L_A the loading rate for species A. The loss rate coefficient α_A in the second term of Eq. 3 characterizes trap loss by collisions with background particles. Inelastic binary collisions between trapped particles are described by the last two terms in Eq. 3. The rate coefficients β_A and γ_{AB} denote the loss rate coefficient for collisions between atoms of the same species and between different atomic species, respectively. These coefficients can be expressed in terms of trap-loss cross sections $\beta_A = \bar{v}_{AA}\sigma_A$ and $\gamma_{AB} = \bar{v}_{AB}\sigma_{AB}$ where \bar{v}_{AA} and \bar{v}_{AB} denote the relative speed between two atoms of species A and between species A and B, respectively.

The rate coefficients for trap loss in Eq. 3 can be inferred from the decay of the fluorescence signal after interruption of the loading flux for species A ($L_A = 0$ in Eq. 3). Species B is still continuously loaded into the two-species MOT ($L_B \neq 0$). The fluorescence signal from the MOT is proportional to the particle number when the cloud of trapped atoms is not optically thick which is well fulfilled in all our measurements. Analysis of the data is simplified by the fact that, for low numbers of trapped particles, the cloud extension is determined solely by the temperature (*temperature-limited regime*) [23]. In this regime, the root-mean-square radius r_A of the Gaussian spatial density distribution is independent of the number of particles which we have carefully checked for our two-species MOT [24]. Thus, the quadratic loss term can be written as $-\beta_A N_A^2 / \sqrt{8V_A}$ where we call $V_A = (\sqrt{2\pi}r_A)^3$ the volume of the species A cloud. The volume V_A stays constant during the decay of the trapped particle number. In addition, the Li cloud is generally much larger than the Cs cloud (see Fig. 4). The third term in Eq. (3) therefore simplifies to $-\gamma \hat{n}_{Li} N_{Cs}$ where $\hat{n}_{Li} = N_{Li}/V_{Li}$ denotes the Li peak density.

With these simplifications, the decay of the trapped particle number N_A is described by

$$\frac{dN_A}{dt} = - \left(\alpha_A + \frac{\gamma_{AB}}{V_{Li}} N_B \right) N_A - \frac{\beta_A}{\sqrt{8V_A}} N_A^2 \quad (4)$$

where A and B stand for Li or Cs. In the general case, N_A and N_B are coupled by the inelastic inter-species collisions (see Fig. 5). However, when the loading flux for species B is large compared to the loss rate by inter-species collisions, i.e. $L_B \gg \gamma_{BA} N_A N_B / V_{Li}$, the steady-state particle number $N_{B,0}$ is not influenced by the presence of species

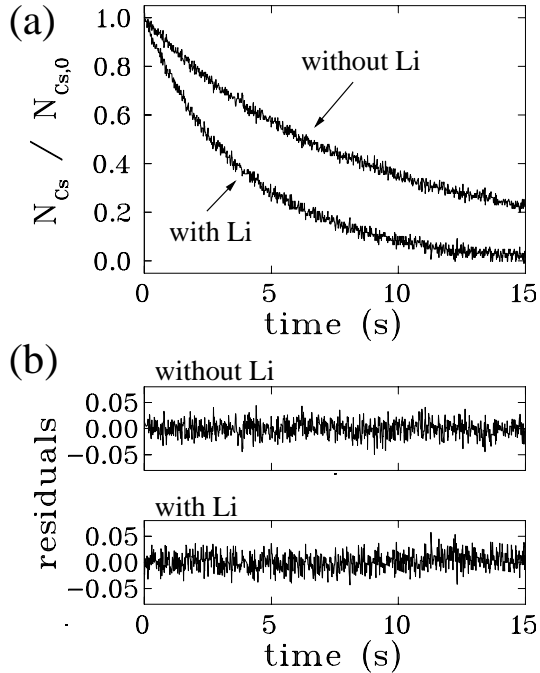


Fig. 6. Decay of fluorescence for Cs in the two-species MOT with and without trapped Li ($\delta_{\text{Cs}} = -1.5 \Gamma_{\text{Cs}}$, $\delta_{\text{Li}} = -3 \Gamma_{\text{Li}}$). The fluorescence signal is proportional to the number of trapped atoms N_{Cs} . The lower graphs show the residuals from a fit to Eq. 5.

A. In this case, the rate equations for A and B become decoupled, and Eq. 4 has the simple analytical solution

$$N_{\text{A}}(t) = \frac{N_{\text{A},0} e^{-\tilde{\alpha}_{\text{A}} t}}{1 + \frac{N_{\text{A},0} \beta_{\text{A}}}{\sqrt{8} V_{\text{A}} \tilde{\alpha}_{\text{A}}} (1 - e^{-\tilde{\alpha}_{\text{A}} t})} \quad (5)$$

with the effective decay rate coefficient $\tilde{\alpha}_{\text{A}} = \alpha_{\text{A}} + \gamma_{\text{AB}} N_{\text{B},0} / V_{\text{Li}}$.

The coefficients α_{A} and β_{A} in Eq. (4) are determined by fitting Eq. (5) to the fluorescence decay *without* the species B loaded into the MOT ($N_{\text{B},0} = 0$). A typical example is depicted in Fig. 6. We have found no influence of the trapping light for species B on the rate coefficients for species A. However, to exclude any possible ambiguities, the trapping light for species B is not interrupted during the measurements without species B being loaded into the trap. In addition, we observe no influence of the species B atomic beam on the decay characteristics of species A when opening the beam shutter and interrupting one arm of the MOT laser beams so that no species B atoms are trapped.

As shown in Fig. 6, the fluorescence decay changes significantly when the second species is also confined in the two-species MOT. By adjusting the loading fluxes, the particle number $N_{\text{B},0}$ is decoupled from the decay of species A which is checked by monitoring the fluorescence of species B. Besides the initial particle number $N_{\text{A},0}$, the inter-species rate coefficient γ_{AB} is the only free fitting parameter used since the single-species parameters α_{A} and β_{A} are kept fixed to the values determined without B.

In this way, determination of γ_{AB} is uncorrelated to the evaluation of α_{A} and β_{A} which greatly reduces the fitting errors.

Experimental errors in the determination of the particle numbers $N_{\text{A},0}$ and $N_{\text{B},0}$ are 25%, while the trap volumes V_{A} and V_{B} are accurate to within 15%. The errors given in the following refer to the combination of experimental errors with the statistical errors of the fitting procedures. Not included are possible systematic errors in the particle number determination which we estimate to about 50%. Comparison of the values for β_{A} from our measurements with previous values measured in single-species MOTs provide a consistency check for our data analysis and the influence of systematics.

4.2 Lithium-induced cesium loss

Following the procedures described in the preceding section, we have studied the trap loss of Cs atoms resulting from inelastic Li-Cs collisions. Li and Cs are loaded for about 30 s to their steady-state particle numbers ($N_{\text{Cs},0} \simeq 10^6$ at $\delta_{\text{Cs}} = -1.5 \Gamma_{\text{Cs}}$, $N_{\text{Li},0} \approx 10^8$ at $\delta_{\text{Li}} = -3 \Gamma_{\text{Li}}$). The decay of the Cs fluorescence is monitored with and without Li after the Cs loading flux is interrupted. In addition, the Li fluorescence is observed during the decay of the Cs fluorescence to verify that $N_{\text{Li},0}$ is independent of N_{Cs} . For each set of measurements, a camera picture is taken to measure the spatial volume V_{Li} of the Li cloud.

We first investigate the influence of the population of the lithium $2P_{3/2}$ excited state on γ_{CsLi} . After the Cs loading is interrupted, the average Li excitation is adjusted by periodically chopping the trapping light. The chopping frequency of 100 kHz is slow compared to the internal dynamics of the Li atoms determined by Γ_{Li} , but fast compared to the dynamics of the trapped particles. Therefore, the average excitation of the Li atoms scales linearly with the ratio of the on/off time intervals (duty cycle)². At 100% duty cycle (no chopping), the average excited-state population \bar{I}_{Li^*} is 0.06(1) at a detuning $\delta_{\text{Li}} = -3 \Gamma_{\text{Li}}$. To determine the population, the fluorescence rate is measured as the function of detuning for a fixed number of trapped atoms. The excited-state population is then deduced from two-level theory by fitting a Lorentzian to the data. The volume V_{Li} of the Li MOT increases with decreasing duty cycle from 1.3(1) mm³ at 100% duty cycle to 3.0(3) mm³ at 30%. The Li temperature does not change significantly with the duty cycle ($T_{\text{Li}} = 0.9(2)$ mK at $\delta_{\text{Li}} = -3 \Gamma_{\text{Li}}$).

The data presented in the left graph of Fig. 7 show that the Cs loss rate coefficient γ_{CsLi} has the constant value of $\gamma_{\text{CsLi}} = 1.1(2) \times 10^{-10}$ cm³/s at $\delta_{\text{Cs}} = -1.5 \Gamma_{\text{Cs}}$ and $\delta_{\text{Li}} = -3 \Gamma_{\text{Li}}$. The coefficient exhibits no significant dependence on the Li excitation. This observation can be regarded as

² The Li loading rate changes with the duty cycle resulting in a decay of $N_{\text{Li},0}$ to a new steady-state value. Therefore, Eq. 5 can not be used in this measurement. The Li decay is measured by monitoring the Li fluorescence. The observed decay of $N_{\text{Li},0}$ is incorporated into Eq. 4.

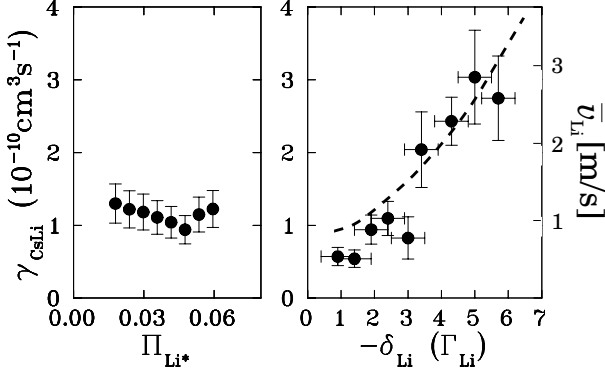


Fig. 7. Left graph: Rate coefficient for lithium-induced cesium loss γ_{CsLi} as a function of the lithium population of the excited $2P_{3/2}$ state ($\delta_{\text{Cs}} = -1.5 \Gamma_{\text{Cs}}$, $\delta_{\text{Li}} = -3 \Gamma_{\text{Li}}$). The excitation was controlled by square-wave modulation of the lithium trapping light. Right graph: Rate coefficient for lithium-induced cesium loss as a function of the lithium detuning δ_{Li} ($\delta_{\text{Cs}} = -1.5 \Gamma_{\text{Cs}}$). The dashed line corresponding to the right abscissa shows the variation of the mean lithium velocity \bar{v}_{Li} with detuning.

a direct consequence of the repulsive interaction between excited Li and ground-state Cs as discussed in Sec. 2.3. Excited Li in the MOT therefore does not contribute to the trap loss of Cs.

In a second set of measurements, the dependence of γ_{CsLi} on the detuning δ_{Li} of the trapping light for Li is investigated. As shown in the right graph of Fig. 7, the interspecies rate coefficient steadily increases with increasing detuning from $0.6(1) \times 10^{-10} \text{ cm}^3/\text{s}$ at $\delta_{\text{Li}} = -1 \Gamma_{\text{Li}}$ to $3.0(6) \times 10^{-10} \text{ cm}^3/\text{s}$ at $\delta_{\text{Li}} = -6 \Gamma_{\text{Li}}$. Changing δ_{Li} has two major consequences: the temperature of Li increases with increasing detuning as demonstrated in [19], and the excitation probability for Li is modified. The dashed line in Fig. 7 gives the dependence of $\bar{v}_{\text{Li}} = (\frac{8}{3} k_B T_{\text{Li}}/m_{\text{Li}})^{1/2}$ on the Li detuning as measured for our Li MOT [19]. As discussed in Sec. 2.3, the Li velocity determines the average relative velocity between lithium and cesium $\bar{v}_{\text{LiCs}} \approx \bar{v}_{\text{Li}}$. Since the change in \bar{v}_{Li} essentially reproduces the measured trend of the rate coefficient, it follows that the cross section $\sigma_{\text{CsLi}} = \gamma_{\text{CsLi}}/\bar{v}_{\text{CsLi}}$ for Li-induced Cs loss is independent on the Li detuning ($\sigma_{\text{CsLi}} = 0.7(2) \times 10^4 \text{ \AA}^2$ at $\delta_{\text{Cs}} = -1.5 \Gamma_{\text{Cs}}$). The data again indicate that the Li excitation plays no role in inelastic Li-Cs collisions.

The rate coefficient $\gamma_{\text{CsLi}} = 1.1(2) \times 10^{-10} \text{ cm}^3/\text{s}$ at $\delta_{\text{Cs}} = -1.5 \Gamma_{\text{Cs}}$ is about one order of magnitude larger than the homonuclear coefficient $\beta_{\text{Cs}} = 2.0(4) \times 10^{-11} \text{ cm}^3/\text{s}$ measured under the same conditions but without lithium in the trap [24]³. The corresponding cross sections $\sigma_{\text{CsLi}} = 0.7(2) \times 10^4 \text{ \AA}^2$ and $\sigma_{\text{Cs}} = 2.0(4) \times 10^4 \text{ \AA}^2$, however, are of the same order of magnitude due to the much smaller relative velocities of the Cs atoms (see Sec. 2.3).

To investigate the influence of optical Cs excitation, the detuning δ_{Cs} of the Cs-trapping light is switched to

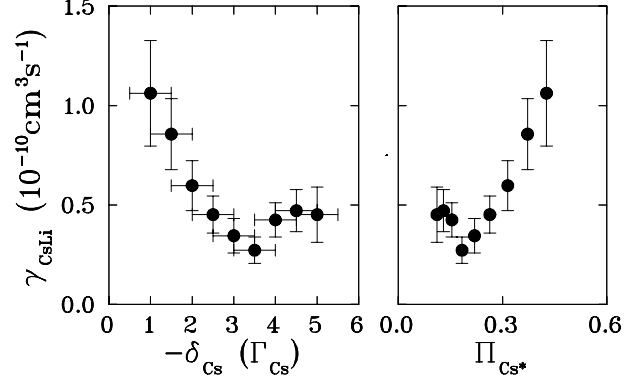


Fig. 8. Left graph: Dependence of the loss rate coefficient for lithium-induced cesium loss γ_{CsLi} on the cesium detuning δ_{Cs} ($\delta_{\text{Li}} = -3 \Gamma_{\text{Li}}$). Right graph: Same data, but plotted versus the average population of the Cs $6P_{3/2}$ state as determined from the detuning.

a given value after interruption of the Cs loading flux. The Li detuning is kept fixed at $\delta_{\text{Li}} = -3 \Gamma_{\text{Li}}$ resulting in a constant number of $N_{\text{Li},0} = 5(2) \times 10^6$ Li atoms at a density $\hat{n}_{\text{Li}} = 1.7(7) \times 10^9 \text{ cm}^{-3}$ in the MOT. As shown in the left graph in Fig. 8, one observes a decrease of the rate coefficient by a factor of five for increasing detuning δ_{Cs} . At higher detuning, γ_{CsLi} rises up again.

Changing the detuning of the Cs MOT has two effects: excitation of the Cs $6P_{3/2}$ state depends on the detuning, and the Cs trap becomes shallower at larger detunings. In addition, the Cs temperature becomes lower at larger detuning due to polarization-gradient cooling [20], but this does not effect the rate coefficient since the relative velocity is determined by the Li temperature only. The increase of the rate coefficient at $-\delta_{\text{Cs}} \geq 4 \Gamma_{\text{Cs}}$ can be attributed to the decrease of the MOT depth. The MOT might eventually become shallow enough to allow for trap loss due to Li-Cs collisions changing the Cs hyperfine structure. From a simplified yet realistic picture for the capture range of the Cs MOT [25], we expect this process to become relevant at detunings below $\approx -4 \Gamma_{\text{Cs}}$ consistent with the observed increase of γ_{CsLi} . The decrease of γ_{CsLi} with detuning for $-\delta_{\text{Cs}} \leq 4 \Gamma_{\text{Cs}}$, however, must be related to the change in the Cs excitation.

The average population of the Cs in the $P_{3/2}$ state in the MOT decreases with the detuning. As described in Sec. 2.2, the relevant inelastic processes for trap loss occur at internuclear distances around 10 \AA . Due to the large relative velocities of about 1 m/s , excitation of Cs survives over an internuclear distance of about 300 \AA . The Cs atoms might therefore be excited at separations before the interatomic interaction energy becomes relevant ($R_C \approx 100 \text{ \AA}$), and still reach the inner interaction zone. The modification of the excitation probability by the interaction potential therefore plays a minor role for the probability for an excited atom to reach the inner interaction zone in the excited state. It seems therefore appropriate to expect a linear increase of γ_{CsLi} with the average excited state population in the MOT.

³ The value of β_{Cs} is consistent with earlier measurements in a Cs MOT by Sesko *et al.* [5].

To support this picture, the right graph in Fig. 8 shows the same data as in (a), but now plotted versus the average population \bar{I}_{Cs^*} of the Cs $P_{3/2}$ state. The excited-state population is measured as described above for Li. The rate coefficient scales proportional to the average $P_{3/2}$ population indicating that excitation relevant for the inelastic processes indeed occurs at large internuclear distances where the modification of the energy through the quasi-molecular potential can be neglected. In addition, the rapid decrease of the rate coefficient with decreasing Cs excitation shows, that inelastic Li-Cs* collisions are the main channel for Li-induced Cs trap loss.

The strong decrease of the rate coefficient with increasing detuning constitutes an important difference to homonuclear collisions where the trap loss rate is found to increase with increasing detuning [5]. In the homonuclear case, the colliding atoms are decoupled from the light field already at distances around 1000 Å due to the long-range resonant-dipole interaction. The rate coefficient for homonuclear collisions can be increased by primarily exciting the atoms at smaller internuclear separations, i.e. at larger detunings from resonance for the attractive interaction potential, resulting in a larger survival probability.

4.3 Cesium-induced lithium loss

The investigation of Cs-induced Li loss from the MOT proceeds similar to the experiments on Li-induced Cs loss. Cesium is permanently loaded, and at a given moment the Li loading flux is interrupted for a measurement of the Li trap decay. It has now to be ensured that the steady-state number $N_{\text{Cs},0}$ of trapped Cs is independent of the number of trapped Li N_{Li} , i.e., the Cs loading rate has to be chosen large compared to the Li-induced Cs loss rate. By decreasing the Li loading flux, the steady-state Li particle number in the MOT is adjusted to values comparable to the largest achievable Cs particle number ($N_{\text{Li},0} \approx N_{\text{Cs},0} \approx 10^6$). Under these conditions, the Cs fluorescence shows only a marginal dependence on the number of trapped Li atoms so that Eq. 5 can be used to analyze the data. At the corresponding low Li densities, the decay of the Li fluorescence was found to be purely exponential indicating that quadratic Li loss can be neglected ($\beta_{\text{Li}} N_{\text{Li},0} / \sqrt{8} V_{\text{Li}} \ll \alpha_{\text{Li,eff}}$ in Eq. 5).

From energetical considerations discussed in Sec. 2.3, trap escape of a Cs atom through an inelastic Li-Cs collision has to be accompanied by the loss of the involved Li atom, since the largest share of the released energy is taken by the Li. In Fig. 9, the ratio between the loss rate coefficient for a Cs-induced Li loss γ_{LiCs} and the coefficient for a Li-induced Cs loss γ_{CsLi} is depicted as function of the Li detuning δ_{Li} . For $-\delta_{\text{Li}} \geq 3\Gamma_{\text{Li}}$ one observes $\gamma_{\text{LiCs}} \approx \gamma_{\text{CsLi}}$, which shows that both collisions partners simultaneously leave the trap. Since the Cs trap escape is essentially determined by collisions involving excited Cs, this collision channel is also the main source for Li loss.

Interestingly, at smaller detunings, an additional loss channel for Li atoms opens which is not accompanied by

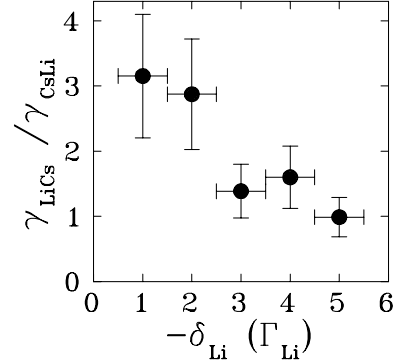


Fig. 9. Ratio between the loss coefficients for cesium-induced lithium loss γ_{LiCs} and lithium-induced cesium loss γ_{CsLi} versus lithium detuning δ_{Li} ($\delta_{\text{Cs}} = -1.5 \Gamma_{\text{Cs}}$).

the loss of the Cs atoms. A possible process releasing sufficient energy for the escape of Li without providing enough energy for Cs is represented by inelastic collisions between Cs and Li both in the ground state (hyperfine-changing collisions, see Sec. 2.2). In particular, in the MOT nearly all ground-state Cs atoms occupy the $6S_{1/2}(F=4)$ level. Collisions changing the hyperfine state of the Cs would transfer around $h \times 9$ GHz of energy to the Li atom, which corresponds roughly to the Li trap depth at small detunings⁴.

To further investigate the hypothesis that the additional Li loss is a manifestation of hyperfine-changing collisions, we have changed the Li trap depth by square-wave modulation of the Li trapping light [26] as explained in the preceding section. At full duty cycle, the trap depth is estimated from the laser power to be around 15 GHz. Lowering the duty cycle thus reduces the trap depth sufficiently to allow for the onset of loss through hyperfine-structure change of the Cs ground state. As shown in Fig. 10 for $\delta_{\text{Li}} = -4 \Gamma_{\text{Li}}$, the loss rate coefficient for Cs-induced Li loss γ_{LiCs} drastically increases when the duty cycle is reduced below a critical value of $\approx 40\%$. At a duty cycle of 20%, a rate coefficient of $\gamma_{\text{LiCs}} = 5(1) \times 10^{-10} \text{ cm}^3/\text{s}$ is measured, corresponding to a cross section of $\sigma_{\text{LiCs}} = 3(1) \times 10^4 \text{ \AA}^2$.

The square-wave modulation method has formerly been used to identify fine-structure changing collisions in a pure Li MOT which releases 5 GHz energy to each Li collision partner [26]. In these experiments, a sudden increase of the rate coefficient β_{Li} with decreasing duty cycle was observed when the duty cycle was lowered beyond the value corresponding to 5 GHz trap depth. We have performed equivalent measurements on β_{Li} for the same trap parameters as the data set shown in Fig. 10, but with maximum Li loading flux to achieve large numbers of trapped Li ($N_{\text{Li},0} \approx 10^8$). This leads to a measurable influence of β_{Li} on the trap loss [24]. The rate coefficient β_{Li} increases from $5(2) \times 10^{-12} \text{ cm}^3/\text{s}$ for duty cycles between 60% and 100% to $\sim 1 \times 10^{-10} \text{ cm}^3/\text{s}$ at duty cycles below

⁴ For Li, the trap depth steadily increases with detuning in the parameter ranges considered here [19].

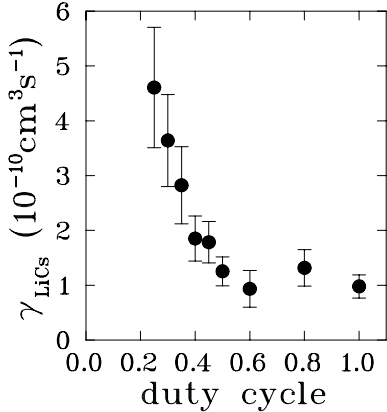


Fig. 10. Loss rate coefficient of cesium-induced lithium loss γ_{LiCs} versus the duty cycle of square-wave modulation of the trap light ($\delta_{\text{Cs}} = -3\Gamma_{\text{Cs}}$, $\delta_{\text{Li}} = -4\Gamma_{\text{Li}}$).

40%⁵. We find that the sudden increase in β_{Li} sets in at a slightly lower critical duty cycle than the increase of γ_{LiCs} shown in Fig. 10. This indicates, that the corresponding kinetic energy gain transferred to the lithium through an inelastic ground-state Li-Cs collisions must be larger than $h \times 5 \text{ GHz}$. The only process releasing sufficient energy to explain the observations is therefore an inelastic collision changing the Cs hyperfine state. Note, that inelastic Li*-Cs collisions changing the Li excited-state fine structure, which would release $h \times 10 \text{ GHz}$ and which are relevant for trap loss through inelastic Li*-Li collisions [26, 27], are excluded by the repulsive quasi-molecular potential (see Sec. 2.3).

5 Conclusions

Our results can be summarized in the following picture of binary inelastic Li-Cs collisions in a combined magneto-optical trap. Lithium and cesium approach each other with a mean relative velocity $\approx 1 \text{ m/s}$ which is determined by the lithium temperature. Since the MOT is operated with near resonant light, atoms can absorb a trapping photon when the interaction energy is still small compared to $\hbar\delta$, i.e. at internuclear separations larger than the Condon point at about 100 \AA .

When the lithium absorbs a trapping photon at 671 nm , the excited Li and ground-state Cs repel each other and inelastic processes are prevented (optical shielding). The rate coefficient for trap loss by Li-Cs collisions is therefore found to be independent of the average Li excitation in the two-species MOT. When a 852 nm -photon is absorbed by the Cs, Li and Cs* are accelerated by the attractive molecular potential. Due to the comparatively large relative velocity, the Cs excitation survives over distances around 300 \AA . The probability is therefore high to reach very

⁵ These values are consistent with rate coefficients from Li-MOT measurements by Kawanake *et al.* [26] and Ritchie *et al.* [27].

small internuclear distances in the excited state. The excited quasi-molecular wavepacket might even oscillate for some periods in the molecular potential well before spontaneous emission occurs. Inelastic Li-Cs processes such as changes of the Cs fine-structure state or the spontaneous emission of a red-detuned photon are then likely to take place. Both processes release sufficient energy for the escape of both atoms from the trap, and our trap loss experiments do not distinguish among them. The cross section for such inelastic Li-Cs* collisions scales with the average Cs excitation in the MOT, and acquires a value of $\sigma_{\text{CsLi}} = \sigma_{\text{LiCs}} = 0.7(2) \times 10^4 \text{ \AA}^2$ at maximum excited-state populations around $\frac{1}{2}$, which corresponds to a trap loss rate coefficient of $\gamma_{\text{CsLi}} = \gamma_{\text{LiCs}} = 1.1(2) \times 10^{-10} \text{ cm}^3/\text{s}$.

Collisions involving lithium and cesium in the ground state generally do not transfer sufficient energy to overcome the trap energy barrier. If, however, the lithium trap depth is decreased below $\approx 9 \text{ GHz}$, lithium atoms eventually escape from the trap after having undergone a Li-Cs collision in which the cesium changes its hyperfine ground state. The cesium atom will be retained in the trap since only 5% of the released energy is transferred to the cesium. Our measurements yield a cross section larger than $\sigma_{\text{LiCs}} = 3 \times 10^4 \text{ \AA}^2$ for a ground-state Li-Cs collision with change of the Cs hyperfine state. The lower bound for the corresponding rate coefficient is $\gamma_{\text{LiCs}} = 5(1) \times 10^{-10} \text{ cm}^3/\text{s}$.

Homonuclear Cs trap loss collisions give about the same inelastic cross sections as Li-Cs collisions, while homonuclear Li collisions have a cross section which is more than one order of magnitude smaller. Due to the small extension of the ground-state *and* the excited state interaction potentials, the Li-Cs cross sections are essentially determined by the s-wave contribution. To our best knowledge, the short-range part of the Li-Cs molecular potential has not yet been theoretically investigated. Detailed knowledge on the fine details of the short-distance molecular potential is necessary to perform calculations on the relative importance of fine-structure changing and radiative-escape processes and to estimate trap-loss cross sections.

Our investigations of inelastic processes between lithium and cesium represent an important step towards a new class of experiments with binary atomic mixtures. Such mixtures open new perspectives for collisional studies in conservative potentials like magnetic or optical traps, for the formation and trapping of cold polar molecules through, e.g., photoassociation, or for the investigation of two-species Bose condensates [28]. Starting from our two-species MOT, we plan to transfer the cold lithium and cesium simultaneously into a far-detuned optical dipole trap [29] for the investigation of elastic Li-Cs collisions with the prospect to sympathetically cool lithium with optically cooled cesium [14].

Fruitful discussions with O. Dulieu are gratefully acknowledged. We thank D. Schwalm for his encouragement and support. This work was supported in part by the Deutsche Forschungsgemeinschaft in the frame of the Gerhard-Hess-Programm.

References

1. Extensive reviews are given by P. Julienne, A. Smith, K. Burnett, in *Advances in Atomic, Molecular and Optical Physics* ed. by B. Bederson and H. Walther, Vol. 30 (Academic Press, San Diego 1992), 141; T. Walker, P. Feng, *ibid.*, Vol. 34, (1994) 125; J. Weiner, *ibid.*, Vol. 35, (1995) 45; P.D. Lett, P.S. Julienne, W.D. Phillips, *Ann. Rev. Phys. Chem.* **46**, (1995) 423; K.-A. Suominen, *J. Phys. B* **29**, (1996) 5981; J. Weiner, V.S. Bagnato, S. Zilio, P. S. Julienne *Rev. Mod. Phys.* **71**, (1999) 1.
2. P.D. Lett, W.D. Phillips, L.P. Ratcliff, S.L. Rolston, M.E. Wagshull, *Phys. Rev. Lett.* **71**, (1993) 2200; J. Miller, R. Cline, D.J. Heinzen, *ibid.*, 2204.
3. W.I. McAlexander, E.R.I. Abraham, R.G. Hulet *Phys. Rev. A* **54**, (1996) R5.
4. M. Prentiss, A. Cable, J. Bjorkholm, S. Chu, E. Raab, D. Pritchard, *Opt. Lett.* **13**, (1988) 452.
5. D. Sesko, T. Walker, C. Monroe, A. Gallagher, C. Wieman, *Phys. Rev. Lett.* **63**, (1989) 961.
6. S. Bali, D. Hoffmann, T. Walker, *Europhys. Lett.* **27**, (1994) 273.
7. A. Fioretti, D. Comparat, A. Crubellier, O. Dulieu, F. Masnou-Seewes, P. Pillet, *Phys. Rev. Lett.* **80**, (1998), 4402; T. Takekoshi, B.M. Patterson, R.J. Knize, *Phys. Rev. Lett.* **81**, (1998) 5105; A. N. Nikolov, E. E. Eyler, X. T. Wang, J. Li, H. Wang, W. C. Stwalley, P. L. Gould, *Phys. Rev. Lett.* **82**, (1999) 703.
8. Simultaneous trapping of two different Rb isotopes is reported by W. Süptitz, G. Wokurka, F. Strauch, P. Kohns, W. Ertmer, *Opt. Lett.* **19**, (1994) 1571.
9. S.D. Gensemer, P.L. Gould, *Phys. Rev. Lett.* **80**, (1998) 936; C. Orzel, S.D. Bergeson, S. Kulin, S.L. Rolston, *ibid.*, 5093.
10. P.S. Julienne, J. Viguè, *Phys. Rev. A* **44**, (1991) 4464.
11. M.S. Santos, P. Nussenzveig, L.G. Marcassa, K. Helmerston, J. Fleming, S.C. Zilio, V.S. Bagnato, *Phys. Rev. A* **52**, (1995) R4340; G.D. Telles, L.G. Marcassa, S.R. Muniz, S.G. Miranda, A. Antunes, C. Westbrook, and V.S. Bagnato, *Phys. Rev. A* **59**, (1999) R23.
12. W. Scherf, V. Wippel, T. Fritz, D. Gruber, L. Windholz, poster presented at the 6th EPS Conference on Atomic and Molecular Physics 1998, *Europhys. Conf. Abstr.* **22D**, (1998) p. 6-31.
13. J.P. Shaffer, W. Chapulpczak, N.P. Bigelow, *Phys. Rev. Lett.* **82**, (1999) 1124; J.P. Shaffer, W. Chapulpczak, N.P. Bigelow, preprint (1998).
14. H. Engler, I. Manek, U. Moslener, M. Nill, Yu.B. Ovchinnikov, U. Schlöder, U. Schünemann, M. Zielonkowski, M. Weidemüller, R. Grimm, *Appl. Phys. B* **67**, (1998) 709.
15. S.K. Sekatskii, *JETP Lett.* **62**, (1995) 916; S.K. Sekatskii and J. Schmiedmayer, *Europhys. Lett.* **36**, (1996) 407.
16. B. Bussery, Y. Achkar, M. Aubert-Frecon, *Chem. Phys.* **116**, (1987) 319.
17. A. Gallagher, D.E. Pritchard, *Phys. Rev. Lett.* **63**, (1989) 957.
18. C. Vadla, C.-J. Lorenzen, K. Niemax, *Phys. Rev. Lett.* **51**, (1983) 988.
19. U. Schünemann, H. Engler, M. Zielonkowski, M. Weidemüller, R. Grimm, *Opt. Comm.* **158**, (1998) 263.
20. A.M. Steane, M. Chowdhury, C.J. Foot, *J. Opt. Soc. Am. B* **9**, (1992) 2142.
21. G.C. Bjorklund, M.D. Levenson, W. Lenth, C. Ortiz, *Appl. Phys. B* **32**, (1983) 145.
22. U. Schünemann, H. Engler, R. Grimm, M. Weidemüller, M. Zielonkowski, *Rev. Scient. Instr.* **70**, (1999) 242 .
23. C.G. Townsend, N.H. Edwards, C.J. Cooper, K.P. Zetie, C.J. Foot, A.M. Steane, P. Szriftgiser, H. Perrin, J. Dalibard, *Phys. Rev. A* **52**, (1995) 1423.
24. U. Schlöder, Diploma thesis, Universität Heidelberg 1998, unpublished.
25. K. Lindquist, M. Stephens, C. Wieman, *Phys. Rev. A* **46**, (1992) 4082.
26. J. Kawanake, K. Shimizu, H. Tanaka, F. Shimizu, *Phys. Rev. A* **48**, (1993) R883.
27. N.W.M. Ritchie, E.R.I. Abraham, Y.Y. Xiao, C.C. Bradley, R.G. Hulet, P.S. Julienne, *Phys. Rev. A* **51**, (1995) 961.
28. C.K. Law, H. Pu, N.P. Bigelow, J.H. Eberly, *Phys. Rev. Lett.* **79**, (1997) 3105; H. Pu, N.P. Bigelow, *Phys. Rev. Lett.* **80**, (1998) 1130; H. Pu, N.P. Bigelow, *ibid.*, 1134.
29. R. Grimm, M. Weidemüller, Yu.B. Ovchinnikov, *Adv. At. Mol. Opt. Phys.*, in press.